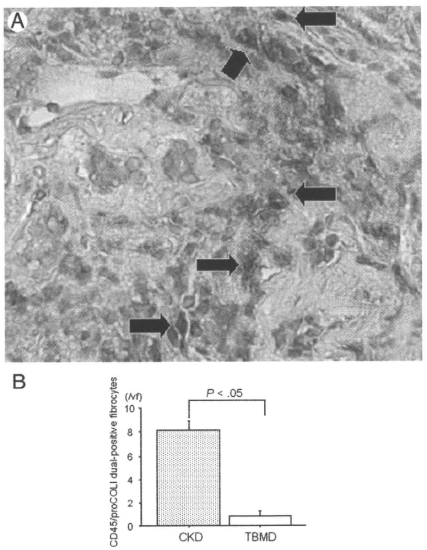

Fig. 1 Immunohistochemical examination of fibrocytes in a representative patient with CKD. A, CD45/proCOLI dual-positive fibrocytes were detected mainly in the interstitium (arrows). CD45 (red) and proCOLI (brown). B, The number of interstitial CD45/proCOLI dual-positive fibrocytes in patients with CKD was higher than that in TBMD patients. Bars indicate means ± SEM.

with CreGN was higher than those in both TBMD and other forms of CKD (Table 1).

3.2. Correlation of fibrocyte infiltration with the pathological findings

The number of infiltrated fibrocytes in the interstitium correlated well with the severity of tubulointerstitial lesions, such as mean interstitial fibrotic area in patients with CKD (r = 0.374, P < .01, Table 2). In addition, there was a significant correlation between the number of interstitial fibrocytes and the number of CD68-positive macrophages in the interstitium (r = 0.386, P < .05, Table 2). On the other hand, fibrocyte infiltration was not significantly correlated with the extent of glomerulosclerosis in CKD patients (Table 2). In patients with CreGN, LN, and DN, the number of interstitial fibrocytes increased with the extent of interstitial fibrosis (r = 0.401, P < .05; r = 0.545, P < .05; r = 0.421, P < .05, respectively). In glomerular lesions, the percentages of fibrocellular/fibrous crescents correlated well with the number of interstitial fibrocytes in CreGN (r = 0.453, P < .05). In patients with LN, the number of fibrocytes in class

Table 2 Correlation of the number of interstitial fibrocytes with pathological findings in CKD

CKD patients	r	P
Glomeruli		
Glomerulosclerosis	0.144	NS
Interstitium		
Fibrosis	0.374	<.01
CD68-positive cells	0.386	<.05

Abbreviations: NS, not significant.

IV was higher than in other forms of LN (11.1 ± 2.7 *vs.* 5.1 ± 1.3 per visual field; P < .05, Fig. 2A). Furthermore, the number of interstitial fibrocytes increased in accordance with the severity of glomerular diffuse lesions (grade I-II, 6.0 ± 1.1; grade III-IV, 10.2 ± 1.0; P < .05, Fig. 2B).

3.3. Correlations between the number of fibrocytes and clinical parameters

In patients with CKD, the number of interstitial fibrocytes increased in accordance with the levels of serum creatinine at the time of biopsy (r = 0.331, P < .05, Table 3). In addition, there was an inverse correlation between the number of interstitial fibrocytes and kidney function determined by creatinine clearance and eGFR at the time of biopsy (r = −0.451, P < .05; r = −0.352, P < .05, Table 3). The levels of C-reactive protein also correlated well with the extent of fibrocyte infiltration (r = 0.317, P < .05, Table 3). Moreover, the levels of urinary CCL2 were significantly correlated with the number of interstitial fibrocytes in patients with CKD (r = 0.637, P < .05). On the other hand, there were no correlations between the number of fibrocytes and the extent of proteinuria, hemoglobin A_{1c} levels, or the levels of urinary CXCL12. Urinary CCL21 protein was not detected in any cases in the present study.

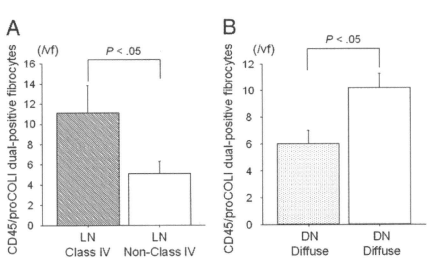

Fig. 2 Increased fibrocytes in the interstitium reflect glomerular lesions in patients with LN and DN. A, The number of interstitial fibrocytes in LN class IV was higher than that in LN non–class IV. B, The number of interstitial fibrocytes increased in accordance with the severity of glomerular diffuse lesions in DN patients. Bars indicate means ± S.E.M.

Table 3 Correlations between the number of interstitial fibrocytes and clinical parameters in CKD

	r	*P*
Proteinuria	0.12	NS
Serum creatinine	0.331	<.05
CRP	0.317	<.05
HbA_{1c}	−0.271	NS
eGFR	−0.352	<.05
Ccr	−0.451	<.05

Abbreviations: Ccr, creatinine clearance; HbA_{1c}, hemoglobin A_{1c}.

3.4. Effects of glucocorticoid therapy on infiltration of fibrocytes and urinary CCL2 levels in patients with CKD

Sixteen of fifty-two patients treated with glucocorticoid therapy received second renal biopsy (CreGN, n = 7; LN, n = 7; IgA-N, n = 2). The number of interstitial fibrocytes decreased significantly during convalescence induced by glucocorticoid therapy including methylprednisolone pulse therapy (before therapy 8.3 ± 1.3 *vs.* after therapy 5.0 ± 1.0, $P < .05$, Fig. 3A). In addition, the number of CD68-positive macrophages in the interstitium also decreased after glucocorticoid therapy (before therapy 11.2 ± 2.8 *vs.* after therapy 5.8 ± 1.1, $P < .05$). Similarly, elevated urinary CCL2 levels significantly decreased during remission induced by glucocorticoid therapy in the patients examined (before therapy 10.7 ± 1.4 *vs.* after therapy 3.1 ± 0.5 pg/mg·creatinine, $P < .05$, Fig. 3B).

4. Discussion

In the present study, we investigated whether fibrocytes participate in the pathogenesis of human CKD. CD45/proCOLI dual-positive fibrocytes were detected in the interstitium in patients with CKD. In addition, the number of interstitial fibrocytes in CKD patients was higher than

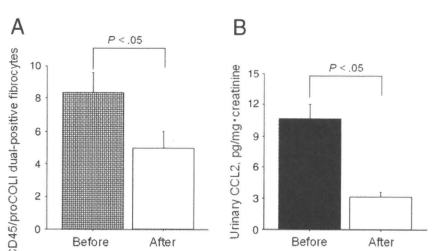

Fig. 3. Changes in the number of fibrocytes in the interstitium (A) and the levels of urinary CCL2 levels (B) after glucocorticoid therapy in patients with CKD. Bars indicate means ± S.E.M.

that in patients with TBMD examined as a disease control. The infiltrated fibrocytes number was well correlated with the extent of interstitial fibrosis. In particular, there were inverse correlations between the number of infiltrated fibrocytes in the interstitium and parameters of kidney function, such as serum creatinine levels, Ccr, and eGFR at the time of biopsy. Taken together, these results suggest that the infiltration of fibrocytes into diseased kidneys may be involved in the pathogenesis of human CKD, especially tubulointerstitial lesions.

Recently, the presence of fibrocytes has been reported in various human fibrotic diseases, including skin, lung, and eye diseases [13,22-24]. In addition, the extent of fibrocyte infiltration into the bronchial mucosa increases in accordance with the severity of persistent airflow obstruction [23]. In fibrotic conditions, the signaling of fibrogenic cytokines such as TGF-β1 has been shown to be involved in the pathogenesis of organ fibrosis, including human kidney disease [25]. Fibrocytes have been demonstrated to produce collagen on stimulation with TGF-β1 [8,13-14]. In this study, the number of interstitial fibrocytes was significantly correlated with the extent of interstitial fibrosis as well as kidney function. These findings suggested that fibrocytes may be involved in the pathogenesis of tubulointerstitial lesions in CKD patients, at least in part, *via* collagen production. On the other hand, TGF-β1 is a well-characterized inducer of EMT in tubular epithelial cells, while bone morphogenic protein-7 counteracts TGF-β1–induced EMT, resulting in improvement of interstitial fibrosis and kidney function in experimental progressive kidney diseases [3]. Recent studies revealed that fibrocytes are capable of producing TGF-β1 under fibrotic conditions [10,15]. Therefore, fibrocytes may regulate EMT through the production of TGF-β1, thereby contributing to the pathogenesis of CKD, in addition to direct synthesis of collagen.

Chemokines are a superfamily of small proteins that are important in recruiting and activating leukocytes during inflammation. Chemokines have been demonstrated to play important roles in the mechanisms of leukocyte entry into the kidneys and the activation of leukocytes in diseased kidneys [26]. CCL2, a member of the CC chemokine family, has been reported to play a significant role in the pathogenesis of human and experimental kidney diseases, especially interstitial fibrosis through recruitment and activation of macrophages [26,27]. In addition, fibrocytes are capable of producing CCL2 [10]. Recent studies also revealed that fibrocytes express various chemokine receptors, including CCR2, a cognate receptor for CCL2 [16]. Furthermore, the expression of type I collagen has been shown to be up-regulated by stimulation with CCL2 in cultured fibrocytes [16]. In this study, we demonstrated that the number of interstitial fibrocytes was well correlated with urinary CCL2 levels as well as the number of interstitial CD68-positive macrophages in patients with CKD. Moreover, glucocorticoid therapy induced reductions in number of fibrocytes and CD68-positive macrophages as well as urinary CCL2 levels.

Taken together, these observations suggest that the CCL2-dependent amplification loop for activation and recruitment of fibrocytes and macrophages may be involved in the pathogenesis of human CKD.

This study demonstrated no association between fibrocyte infiltration and the levels of urinary CXCL12. The CXCL12/CXCR4 pathway has been reported to be involved in the pathogenesis of pulmonary fibrosis through infiltration of fibrocytes [5]. Recently, CXCR4 has been demonstrated to be expressed not only on fibrocytes but also on various cell types, including mesenchymal stem cells [28]. Therefore, CXCL12/CXCR4 signaling may contribute to the mechanisms of disease progression as well as tissue repair. Further studies are required to elucidate the involvement of CCL12/CXCR4 in the pathogenesis of human kidney diseases. Furthermore, urinary CCL21 protein was not detected in any sample in this study. CCL21/CCR7 signaling has been reported to contribute to the migration of fibrocytes leading to tissue fibrosis, including that in the kidney [6,8]. CCL21 is a unique chemokine expressed mainly on vessels, thereby contributing to the infiltration of CCR7-positive cells, such as fibrocytes and dendritic cells [6]. Therefore, it is suggested that CCL21 is hardly secreted into the urine. Further studies of CCL21 expression in human kidney tissues are required.

In this study, the number of interstitial fibrocytes was correlated well with the extent of interstitial fibrosis in patients with CreGN, LN, and DN. Recent studies revealed that mitogen-activated protein kinases (MAPKs) contribute to the pathogenesis of tubulointerstitial lesions in progressive kidney diseases, such as CreGN, LN, and DN [29-31]. To date, at least 3 distinct groups of MAPKs have been identified: extracellular signal-regulated kinases, p38MAPK, and c-Jun NH2-terminal kinase/stress-activated protein kinase. Especially, p38MAPK is phosphorylated in response to hyperosmolarity, oxidative stress, and inflammatory cytokines, thereby contributing to the activation of nuclear transcription factors, including nuclear factor-κB, which principally regulates the gene expression of various chemokines, such as CCL2 [31]. In addition, the expression of type I collagen is also regulated by the MAPK family in cultured fibrocytes [32]. Taken together, these observations suggest that fibrocytes regulated by MAPKs may be involved in the pathogenesis of CKD. Further studies are needed to elucidate the effects of MAPKs on fibrocytes in CKD. In this study, little infiltration of fibrocytes into glomeruli was detected. In addition, the number of interstitial fibrocytes was not correlated with the index of glomerulosclerosis in all patients with CKD. However, the extent of fibrocyte infiltration in the interstitium was correlated with the percentages of fibrocellular/fibrous crescents in CreGN patients. The number of interstitial fibrocytes also increased in accordance with the progression of glomerular lesions in LN and DN patients. These findings suggest that fibrocytes are not directly involved in the pathogenesis of glomerular injury in patients with CKD, while fibrocyte infiltration in the interstitium may reflect the activity and phase of glomerular lesions in CreGN, LN, and DN.

The clinical management of CKD remains to be investigated due to a lack of effective treatment or accurate indicators of disease progression. Previous clinical studies have shown that the renin-angiotensin system (RAS) is a major pathway involved in the pathogenesis of cardiovascular diseases as well as CKD [33,34]. A recent study indicated the expression of two isoforms of angiotensin II receptor (AT1 and AT2) and the effects of RAS on the expression of COLAI as well as TGF-β1 in cultured fibrocytes [15]. Therefore, the effects of RAS on the pathogenesis of CKD may be mediated, in part, by regulation of fibrocytes. Further studies are required to elucidate the interaction of fibrocytes with RAS in CKD. In this study, there was an inverse correlation between the number of interstitial fibrocytes and kidney function. In addition, fibrocytes numbers in peripheral blood have been reported to predict early mortality in patients with idiopathic pulmonary fibrosis and increase in accordance with the severity of asthma [23,35]. Taken together, these observations suggest that the number of fibrocytes in clinical samples may be useful as a biomarker for the progression of organ fibrosis. However, additional investigations are needed to determine the role of fibrocytes in CKD.

In summary, our results suggested that the pathogenesis of human CKD may be closely related to fibrocyte infiltration, which may be regulated by CCL2. In addition, fibrocytes may be a novel therapeutic target for human CKD.

References

[1] Stenvinkel P, Carrero JJ, Axelsson J, et al. Emerging biomarkers for evaluating cardiovascular risk in the chronic kidney disease patient: how do new pieces fit into the uremic puzzle? Clin J Am Soc Nephrol 2008;3:505-21.

[2] Nath KA. The tubulointerstitium in progressive renal disease. Kidney Int 1998;54:992-4.

[3] Zeisberg M, Hanai J, Sugimoto H, et al. BMP-7 counteracts TGF-beta1-induced epithelial-to-mesenchymal transition and reverses chronic renal injury. Nat Med 2003;9:964-8.

[4] Kitagawa K, Wada T, Furuichi K, et al. Blockade of CCR2 ameliorates progressive fibrosis in kidney. Am J Pathol 2004;165:237-46.

[5] Phillips RJ, Burdick MD, Hong K, et al. Circulating fibrocytes traffic to the lungs in response to CXCL12 and mediate fibrosis. J Clin Invest 2004;114:438-46.

[6] Sakai N, Wada T, Yokoyama H, et al. Secondary lymphoid tissue chemokine (SLC/CCL21)/CCR7 signaling regulates fibrocytes in renal fibrosis. Proc Natl Acad Sci U S A 2006;103:14098-103.

[7] Kisseleva T, Uchinami H, Feirt N, et al. Bone marrow-derived fibrocytes participate in pathogenesis of liver fibrosis. J Hepatol 2006;45:429-38.

[8] Abe R, Donnelly SC, Peng T, et al. Peripheral blood fibrocytes: differentiation pathway and migration to wound sites. J Immunol 2001;166:7556-62.

[9] Wada T, Sakai N, Matsushima, et al. Fibrocytes: a new insight into kidney fibrosis. Kidney Int 2007;72:269-73.

[10] Chesney J, Metz C, Stavitsky AB, et al. Regulated production of type I collagen and inflammatory cytokines by peripheral blood fibrocytes. J Immunol 1998;160:419-25.
[11] Bucala R, Spiegel LA, Chesney J, et al. Circulating fibrocytes define a new leukocyte subpopulation that mediates tissue repair. Mol Med 1994;1:71-81.
[12] Bucala R. Circulating fibrocytes: cellular basis for NSF. J Am Coll Radiol 2008;5:36-9.
[13] Schmidt M, Sun G, Stacey MA, et al. Identification of circulating fibrocytes as precursors of bronchial myofibroblasts in asthma. J Immunol 2003;171:380-9.
[14] Yang L, Scott PG, Giuffre J, et al. Peripheral blood fibrocytes from burn patients: identification and quantification of fibrocytes in adherent cells cultured from peripheral blood mononuclear cells. Lab Invest 2002;82:1183-92.
[15] Sakai N, Wada T, Matsushima K, et al. The renin-angiotensin system contributes to renal fibrosis through regulation of fibrocytes. J Hypertens 2008;26:780-90.
[16] Moore BB, Kolodsick JE, Thannickal VJ, et al. CCR2-mediated recruitment of fibrocytes to the alveolar space after fibrotic injury. Am J Pathol 2005;166:675-84.
[17] Levey AS, Eckardt KU, Tsukamoto Y, et al. Definition and classification of chronic kidney disease: a position statement from Kidney Disease: Improving Global Outcomes (KDIGO). Kidney Int 2005;67:2089-100.
[18] Yokoyama H, Wada T, Hara A, et al. The outcome and a new ISN/RPS 2003 classification of lupus nephritis in Japanese. Kidney Int 2004;66: 2382-8.
[19] Iseki K, Horio M, Imai E, et al. Geographic difference in the prevalence of chronic kidney disease among Japanese screened subjects: Ibaraki versus Okinawa. Clin Exp Nephrol 2009;13:44-9.
[20] Sakai N, Wada T, Furuichi K, et al. Involvement of extracellular signal-regulated kinase and p38 in human diabetic nephropathy. Am J Kidney Dis 2005;45:54-65.
[21] Wada T, Furuichi K, Segawa-Takaeda C, et al. MIP-1alpha and MCP-1 contribute to crescents and interstitial lesions in human crescentic glomerulonephritis. Kidney Int 1999;56:995-1003.
[22] Ishida Y, Kimura A, Takayasu T, et al. Detection of fibrocytes in human skin wounds and its application for wound age determination. Int J Legal Med 2009;123:299-304.
[23] Saunders R, Siddiqui S, Kaur D, et al. Fibrocyte localization to the airway smooth muscle is a feature of asthma. J Allergy Clin Immunol 2009;123:376-84.
[24] Abu El-Asrar AM, Struyf S, Van Damme J, et al. Circulating fibrocytes contribute to the myofibroblast population in proliferative vitreoretinopathy epiretinal membranes. Br J Ophthalmol 2008;92:699-704.
[25] Hohenstein B, Daniel C, Hausknecht B, et al. Correlation of enhanced thrombospondin-1 expression, TGF-beta signalling and proteinuria in human type-2 diabetic nephropathy. Nephrol Dial Transplant 2008;23: 3880-7.
[26] Wada T, Furuichi K, Sakai N, et al. Gene therapy via blockade of monocyte chemoattractant protein-1 for renal fibrosis. J Am Soc Nephrol 2004;15:940-8.
[27] Wada T, Furuichi K, Sakai N, et al. Up-regulation of monocyte chemoattractant protein-1 in tubulointerstitial lesions of human diabetic nephropathy. Kidney Int 2000;58:1492-9.
[28] Sordi V. Mesenchymal stem cell homing capacity. Transplantation 2009;87:S42-5.
[29] Wada T, Furuichi K, Sakai N, et al. Involvement of p38 mitogen-activated protein kinase followed by chemokine expression in crescentic glomerulonephritis. Am J Kidney Dis 2001;38:1169-77.
[30] Iwata Y, Wada T, Furuichi K, et al. p38 Mitogen-activated protein kinase contributes to autoimmune renal injury in MRL-Fas lpr mice. J Am Soc Nephrol 2003;14:57-67.
[31] Lim AK, Nikolic-Paterson DJ, Ma FY, et al. Role of MKK3-p38 MAPK signalling in the development of type 2 diabetes and renal injury in obese db/db mice. Diabetologia 2009;52:347-58.
[32] Hong KM, Belperio JA, Keane MP, et al. Differentiation of human circulating fibrocytes as mediated by transforming growth factor-beta and peroxisome proliferator-activated receptor gamma. J Biol Chem 2007;282:22910-20.
[33] Pfeffer MA, Swedberg K, Granger CB, et al. Effects of candesartan on mortality and morbidity in patients with chronic heart failure: the CHARM-Overall programme. Lancet 2003;362:759-66.
[34] Brenner BM, Cooper ME, de Zeeuw D, et al. Effects of losartan on renal and cardiovascular outcomes in patients with type 2 diabetes and nephropathy. N Engl J Med 2001;345:861-9.
[35] Moeller A, Gilpin SE, Ask K, et al. Circulating Fibrocytes Are an Indicator for Poor Prognosis in Idiopathic Pulmonary Fibrosis. Am J Respir Crit Care Med 2009;179:588-94.

Clin Exp Nephrol
DOI 10.1007/s10157-010-0372-2

REVIEW ARTICLE

Involvement of bone-marrow-derived cells in kidney fibrosis

Takashi Wada · Norihiko Sakai · Yoshio Sakai · Kouji Matsushima · Shuichi Kaneko · Kengo Furuichi

Received: 30 August 2010 / Accepted: 18 October 2010

Abstract Cellular mechanisms have been proposed in the pathogenesis of fibrotic processes in the kidney. In this setting, cell sources underlying the generation of matrix-producing cells in diseased kidneys have been categorized as activated resident stromal cells (e.g., fibroblasts, pericytes), infiltrating bone-marrow-derived cells (e.g., fibrocytes, T cells, macrophages), and cells derived from epithelial–mesenchymal transition/endothelial–mesenchymal transition. Among these cell sources, accumulating evidence has shed light on the involvement of bone-marrow-derived cells, including monocytes/macrophages, and a circulating mesenchymal progenitor cell, fibrocyte, in the progression of fibrosis in kidney. Bone-marrow-derived cells positive for CD45 or CD34, and type 1 (pro)collagen dependent on the chemokine and renin–angiotensin systems migrate into diseased kidneys and enhance synthesis matrix protein, cytokines/chemokines, and profibrotic growth factors, which may promote and escalate chronic inflammatory processes and possible interaction with resident stromal cells, thereby perpetuating kidney fibrosis.

Keywords Fibrocyte · Chemokine · Fibrosis · Kidney · Fibroblast · Bone-marrow-derived cells

Presented at the 53rd Annual Meeting of the Japanese Society of Nephrology.

T. Wada (✉)
Division of Nephrology, Department of Laboratory Medicine, Institute of Medical, Pharmaceutical and Health Sciences, Faculty of Medicine, Kanazawa University, 13-1 Takara-machi, Kanazawa 920-8641, Japan
e-mail: twada@m-kanazawa.jp

N. Sakai · S. Kaneko
Department of Disease Control and Homeostasis, Institute of Medical, Pharmaceutical and Health Sciences, Faculty of Medicine, Kanazawa University, Kanazawa, Japan

Y. Sakai
Department of Laboratory Medicine, Institute of Medical, Pharmaceutical and Health Sciences, Faculty of Medicine, Kanazawa University, Kanazawa, Japan

K. Matsushima
Department of Molecular Preventive Medicine, University of Tokyo, Tokyo, Japan

K. Furuichi
Division of Blood Purification, Kanazawa University Hospital, Kanazawa, Japan

Introduction

Fibrosis is a characteristic hallmark that determines the prognosis of any kind of progressive kidney disease and leads to kidney failure. The histological characteristics of interstitial fibrosis in the kidney are evidenced by the presence of tubular atrophy and dilation, interstitial leukocyte infiltration, accumulation of fibroblasts, and increased interstitial matrix deposition [1]. In this aspect, there is accumulating evidence that cellular mechanisms driving fibrosis are involved [2]. Cell sources underlying the generation of matrix-producing cells in diseased kidneys have been categorized as follows: (1) activated resident stromal cells (e.g., fibroblasts, pericytes), (2) infiltrating bone-marrow-derived cells (e.g., fibrocytes, T cells, macrophages), (3) epithelial–mesenchymal transition (EMT)/endothelial–mesenchymal transition (EndMT) [3–5] (Fig. 1).

Among cells responsible for kidney fibrosis, fibrocytes, originally identified in 1994 as a circulating bone-marrow-derived $CD34^+$ cell population of fibroblast-like cells, were reported to infiltrate from inflammatory exudates into a

Published online: 10 December 2010

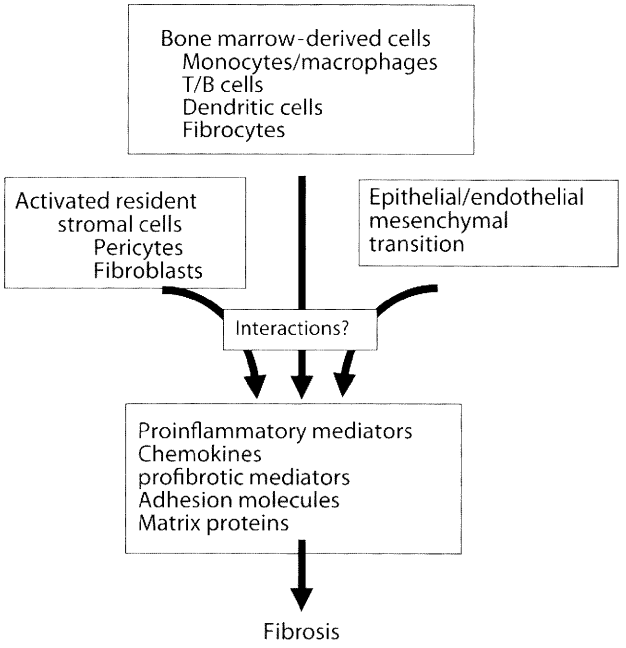

Fig. 1 Possible cellular mechanisms involved in kidney fibrosis

subcutaneously implanted wound chambers [6]. Accumulating evidence suggests that fibrocytes, uniquely comprising a minor fraction of the circulating pool of leukocytes (<1%), are candidates for participating in organ fibrosis associated with conditions in lungs, skin, visceral fibrosis, heart, liver, and kidneys, as well as in physiological roles such as wound repair, cochlear physiology, and auditory function [7, 8]. In addition, a recent study revealed that the delicate balance of peroxisome-proliferator-activated receptor gamma and transforming growth factor (TGF)-beta 1 activation drives the selection of an adipocyte or myofibroblast differentiation pathway through stress-activated protein kinase/c-Jun NH2-terminal kinase (SAPK/JNK) signaling [9]. Originally, fibrocytes were identified by CD34 and collagen-1 coexpression [6, 7]. A recent study revealed that markers (CD45RO, 25F9, S100A8/A9) distinguish monocyte-derived fibrocytes from monocytes, macrophages, and fibroblasts [10]. However, identification of markers specific to fibrocytes remains to be investigated. Fibrocytes may be identified by dual positivity of CD34 or CD45 and collagen-1 or procollagen-1 [6, 7]. In this manuscript, we focus on the involvement of bone-marrow-derived cells in the pathogenesis of kidney fibrosis.

Detection of cells dual positive for CD34 or CD45 and type 1 collagen in kidney fibrosis

The detection and role of fibrocytes in progressive kidney fibrosis remains to be investigated. Using immunostaining and flow cytometry analyses, we uncovered CD45 and type 1 collagen dual-positive ($CD45^+/Col1^+$) cells infiltrating the interstitium, especially the corticomedullary regions, in progressive kidney fibrosis induced by ureteral ligation in mice [11] (Fig. 2a). The number of infiltrating fibrocytes increased with fibrotic progression after ureteral ligation, reaching a peak on day 7 (Fig. 2b). To further verify the existence of fibrocytes, dual immunostainings of CD34 and type 1 collagen were also performed. The infiltration of $CD45^+/Col1^+$ cells was also observed in the interstitium and correlated with disease progression.

These findings prompted us to explore the presence of $CD45^+/proCol1^+$ cells infiltrating into human kidneys, including in people with diabetic nephropathy. The number of infiltrating $CD45^+/proCol1^+$ cells in the interstitium correlated well with the severity of tubulointerstitial lesions, such as interstitial fibrosis, the number of CD68-positive macrophages, and urinary monocyte chemoattractant protein-1 (MCP-1)/chemokine (C-C motif) ligand 2 (CCL2) levels in patients with chronic kidney disease. In particular, there was an inverse correlation between the number of interstitial $CD45^+/proCol1^+$ cells and kidney function at the time of biopsy [12]. The number of interstitial $CD45^+/proCol1^+$ cells and macrophages, as well as urinary MCP-1/CCL2 levels were significantly decreased during convalescence induced by glucocorticoid therapy. Collectively, these results suggest that $CD45^+/proCol1^+$ cells may be involved in the pathogenesis of chronic kidney disease, leading to kidney fibrosis through the interaction with macrophages and MCP-1/CCL2.

Chemokine system involved in infiltration of bone-marrow-derived cells dual positive for CD34 or CD45 and type 1 collagen into kidney

It is of note that fibrocytes isolated from humans and mice express chemokine receptors, such as chemokine (C-C motif) receptor (CCR)2, CCR3, CCR5, CCR7, and CXCR4, thereby regulating the recruitment to sites of fibrosis [7, 11, 13–15]. Supporting this notion, intradermal instillation of secondary lymphoid tissue chemokine (SLC)/CCL21 was first described to induce recruitment of fibrocytes at the injected site [16]. In addition to skin lesions, CCR7-expressing infiltrating cells, also positive for type 1 collagen ($CCR7^+/Col1^+$), were detected in diseased kidneys 7 days after ureteral ligation in wild-type mice [11]. 37.8% of infiltrating cells expressed CCR7 (number of $CCR7^+/Col1^+$ divided by the number of $CCR7^+$ or $CXCR4^+$ or $CCR2^+/Col1^+$). In wild-type mice, the ratio of $CCR7^+/Col1^+$ cells in obstructed kidneys was increased to 7.9% of the total isolated renal cells compared with that in normal (0.25%) and contralateral (0.21%) kidneys. Of these

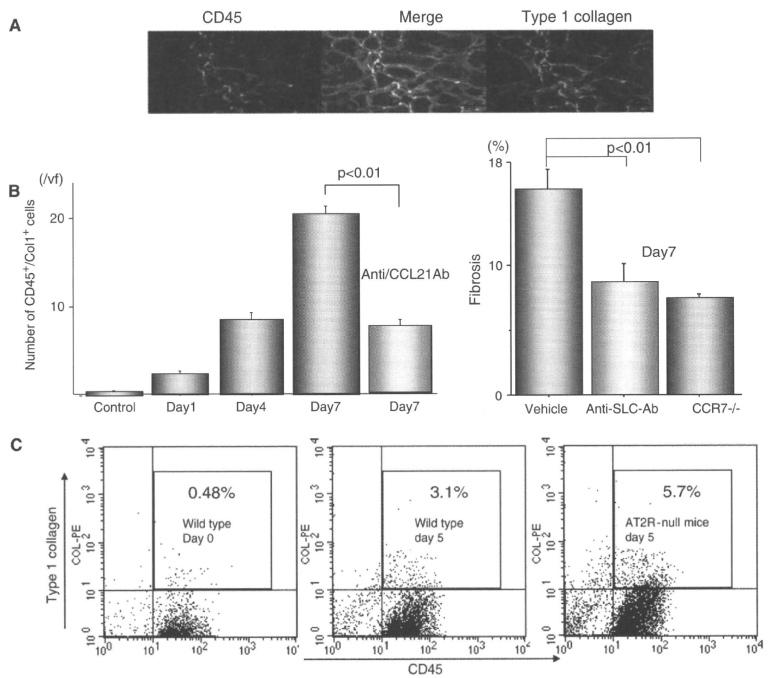

Fig. 2 Cells dual positive for CD34 or CD45 and type 1 collagen ($CD45^+/Col1^+$) cells, detected in kidneys and bone marrow, may play a role in kidney fibrosis. **a** In wild-type mice, $CD45^+/Col1^+$ cells infiltrated the interstitium, especially the corticomedullary regions after ureteral ligation. **b** The number of infiltrating $CD45^+/Col1^+$ cells as well as mean interstitial fibrosis in the kidney were reduced in mice treated with anti-chemokine (C-C motif) ligand 21 (CCL21) antibodies and in chemokine (C-C motif) receptor 7 (CCR7)-null mice compared with that in wild-type mice 7 days after ureteral ligation. Values are mean ± standard error of mean. **c** By flow cytometry analyses, fibrocytes increased in number in bone marrow cells, which were enhanced in angiotensin type 2 receptor (AT2R-null mice with ureteral ligation

CCR7-expressing cells in obstructed kidneys, 66.5% were $CXCR4^+/CCR2^+$, 16.8% were $CXCR4^+/CCR2^-$, 4.3% were $CXCR4^-/CCR2^+$, and 12.4% were $CXCR4^-/CCR2$ cells. The impact of CCL21/CCR7 signaling on progressive kidney interstitial fibrosis was further examined. Mean interstitial fibrosis and the amount of hydroxyproline were reduced by almost 50% in mice treated with anti-CCL21 antibodies compared with that in wild-type mice 7 days after ureteral ligation, which was confirmed by the similar reduction in CCR7-null mice [11]. Accordingly, based on the finding that treatment with anti-CCL21 antibodies or CCR7 deficiency resulted in >50% reduction in the number of $CD45^+/Col1^+$ cells, CCL21/CCR7 signaling is thought to be the major pathway attracting $CD45^+/Col1^+$ cells into the kidney in this particular model [11]. Interestingly, blockade of CCL21/CCR7 signaling reduced the number CCR2-expressing infiltrates in immunohistochemical studies, along with renal transcripts of MCP-1/CCL2. In vitro studies also revealed that stimulation of cultured $CD45^+/Col1^+$ cells with angiotensin II enhanced the expression of messenger RNA (mRNA) of type 1 collagen and TGF-beta [17]. These findings further suggest that $CD45^+/Col1^+$ cells may contribute to kidney fibrosis by producing MCP-1/CCL2 and TGF-beta, which may be responsible for chronic persistent inflammatory processes and activation of resident stromal cells (e.g., fibroblasts, pericytes) and the process to EMT/EndMT, in addition to collagen synthesis of $CD45^+/Col1^+$ cells. All these events may orchestrates downstream

fibrotic events, eventually resulting in kidney fibrosis (Fig. 1).

Renin–angiotensin system and bone-marrow-derived cells dual positive for CD45 and type 1 collagen

The renin–angiotensin system (RAS) is one of the major pathways in the pathogenesis of fibrotic conditions and is possibly dependent on two major distinct receptors, designated as angiotensin II receptor type 1 (AT1R) and angiotensin II receptor type 2 (AT2R). We hypothesized that $CD45^+/Col1^+$ cells might contribute to kidney fibrosis dependent on the RAS. In a murine model, the extent of kidney fibrosis in AT2R-deficient mice was more evident, concomitant with the larger number of infiltrating $CD45^+/Col1^+$ cells in fibrotic kidneys [17]. Interestingly, $CD45^+/Col1^+$ cell numbers in bone marrow were also increased in mice with ureteral ligation, especially in AT2R-deficient mice (Fig. 2c). In the therapeutic points of view, pharmacologic inhibition of AT1R reduced the degree of kidney fibrosis as well as the number of $CD45^+/Col1^+$ cells in both the kidney and bone marrow. AT1R inhibition also decreased the angiotensin-II-stimulated expression of type 1 collagen synthesis in isolated human $CD45^+/Col1^+$ cells, whereas an AT2R inhibitor augmented the expression of mRNA of type 1 collagen. These results suggest that AT1R/AT2R signaling may contribute to the pathogenesis of kidney fibrosis by at least two mechanisms: (1) by regulating the number of $CD45^+/Col1^+$ cells in bone marrow, and (2) by activation of these cells [17].

Fibrocytes: possible clinical biomarker for fibrotic disease

Clinical biomarkers for reflecting fibrogenic activity and indicating disease progression are required in various fields. Moeller et al. reported that fibrocytes defined as cells positive for CD45 and collagen 1 were significantly elevated in patients with stable idiopathic pulmonary fibrosis (IPF), with a further increase during acute disease exacerbation. Fibrocyte numbers were an independent predictor of early mortality. The mean survival of patients with fibrocytes >5% of total blood leukocytes was 7.5 months compared with 27 months for patients with <5%. Thus, the authors concluded that circulating fibrocytes in patients with IPF are an indicator for disease activity of IPF and might be useful as a clinical marker for disease progression [18]. Supporting this notion, the number of interstitial $CD45^+/proCol1^+$ cells was significantly decreased during convalescence induced by glucocorticoid therapy in patients with chronic kidney diseases [12]. Further studies are required to provide evidence that counting fibrocyte numbers might be a biomarker for activity and progression of fibrotic conditions.

Involvement of monocytes/macrophages in kidney fibrosis

Recent studies reveal that macrophage diversity in response to their microenvironment, which uncovers their roles in kidney injury, raising therapeutic possibilities to attenuate kidney fibrosis [19, 20]. In our viewpoint, human peripheral CD14-positive monocytes/macrophages directly contribute to producing type 1 collagen, resulting in fibrogenesis, and are dependent on an amplification loop of MCP-1/CCL2–CCR2 [21]. In addition, the presence of MCP-1/CCL2 expression is suggestive of a chronic stage of disease, especially in tubulointerstitial lesions and urinary levels of protein excretion, despite renal etiologies through the recruitment and activation of macrophages. As is well known, urinary protein excretion promotes and escalates tubulointerstitial lesions, resulting in kidney fibrosis. Moreover, the measurement of urinary MCP-1/CCL2 levels is a useful clinical tool for monitoring the disease activity of inflammatory renal disorders, including diabetic nephropathy [22–25]. This was supported by the fact that blockade of MCP-1/CCL2 prevented leukocyte migration to the kidney, urinary protein excretion, and TGF-beta expression, thereby preventing glomerulosclerosis and interstitial fibrosis [23, 26–28]. In addition to MCP-1/CCL2–CCR2, blockade of fractalkine-CX3CR1 also reduced kidney fibrosis, which was concomitant with reduction in macrophage infiltration [29]. CCR2 receptor is expressed in glomerular podocytes, suggesting MCP-1/CCL2 activation of CCR2 on podocytes may underlie induction of MMP-12, leading to glomerular basement membrane damage and urinary protein excretion [30]. Finally, it is of note that there were significant correlations between the numbers of $CD45^+/proCol1^+$ cells and macrophages in human kidneys as well as urinary levels of MCP-1/CCL2, suggesting the close relationship of $CD45^+/proCol1^+$ cells with macrophages. Based on these results, we propose the MCP-1/CCL2–CCR2 axis on recruitment and activation of bone-marrow-derived cells, especially macrophages, plays a role in the pathogenesis of tubulointerstitial lesions, resulting in kidney fibrosis despite kidney etiologies (Fig. 3).

Involvement of T cells in kidney fibrosis

The degree of fibrosis is related to leukocyte infiltration. Tapmeier et al. [31] examined the role of different T-cell

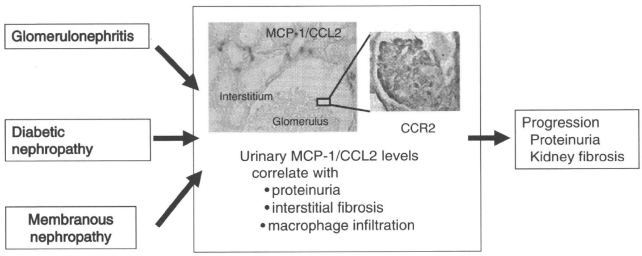

Fig. 3 Macrophages dependent on monocyte chemoattractant protein-1 (MCP-1)/chemokine (C-C motif) ligand 2 (CCL2)–CC receptor 2 (CCR2) axis contribute to progressive kidney diseases, resulting in fibrosis

populations on kidney fibrosis in the mouse model of unilateral ureteral obstruction. They found a critical role for $CD4^+$ T cells in kidney fibrosis. In addition, Nikolic-Paterson [32] describes modulation of T cells in the process of kidney fibrosis: (1) T cells may act directly on fibroblasts and pericytes to promote their migration, proliferation, and differentiation, resulting in accumulation of alpha smooth-muscle actin (SMA^+) myofibroblasts, which synthesize and deposit interstitial matrix; (2) T cells may induce a profibrotic phenotype in the infiltrating macrophage population, which, in turn, secretes profibrotic and pro-proliferative cytokines and growth factors that induce fibroblast migration, proliferation, and differentiation; (3) T cells may act directly on tubular epithelial cells to induce secretion of cytokines and growth factors that, in turn, act on fibroblasts.

Stromal cell activation and myofibroblast generation in kidney fibrosis

Activation of local stromal cells (e.g., fibroblasts and pericytes) and generation of myofibroblasts from epithelial cells (via EMT), pericytes, endothelial cells (via EndMT), and bone-marrow-derived cells are key processes in tubulointerstitial fibrosis [33]. For 15 years, EMT has been viewed as a principle source of fibroblasts in tissue fibrosis [34]. In addition to tubular epithelial cells, glomerular podocytes [35] and endothelial cells [36, 37] undergo transition after injury and have been reported to be involved in kidney damage, resulting in fibrosis. More recently, in the process of perpetuation of fibrogenesis, hypermethylation of *RASAL1*, encoding an inhibitor of the Ras oncoprotein, is associated with the perpetuation of fibroblast activation and fibrogenesis in the kidney [38]. In contrast, Duffiels et al. report that pericytes and perivascular fibroblasts are primary sources of collagen-producing cells in kidney fibrosis [39, 40]. Therefore, further studies are required to determine the degree to which processes including those resulting from bone-marrow-derived cells contribute to kidney fibrosis.

Concluding remarks and future directions

A deep insight into bone-marrow-derived cells dependent on the chemokine and RAS systems provides a key for the novel pathogenesis of progressive organ fibrosis, including kidney fibrosis. In addition to those systems, our recent unpublished data suggest the possible involvement of $CD45^+/Col1^+$ cells in diabetic nephropathy, which is supported by the evidence that $CD45^+/proCol1^+$ cells are detected in human diabetic nephropathy [12]. Further studies for biology of bone-marrow-derived cells and the interaction of resident stromal cells would be required for a better understanding and the therapeutic benefit for kidney fibrosis.

Acknowledgments TW is a recipient of a Grant-in-Aid from the Ministry of Education, Science, Sports and Culture in Japan and Takeda Science Foundation.

References

1. Strutz F, Zeisberg M. Renal fibroblasts and myofibroblasts in chronic kidney disease. J Am Soc Nephrol. 2006;17:2992–8.
2. Wynn TA. Cellular and molecular mechanisms of fibrosis. J Pathol. 2008;214:199–210.
3. Guarino M, Tosoni A, Nebuloni M. Direct contribution of epithelium to organ fibrosis: epithelial–mesenchymal transition. Hum Pathol. 2009;40:1365–76.
4. Vernon MA, Mylonas K, Hughes J. Macrophages and renal fibrosis. Semin Nephrol. 2010;30:302–7.
5. Tapmeier TT, Fearn A, Brown K, Chowdhury P, Sacks SH, Sheerin NS, Wong W. Pivotal role of CD4+ T cells in renal fibrosis following ureteric obstruction. Kidney Int. 2010;78:351–62.
6. Bucala R, Spiegel L, Chesney J, Hogan M, Cerami A. Circulating fibrocytes define a new leukocyte subpopulation that mediates tissue repair. Mol Med. 1994;1:71–81.
7. Herzog EL, Bucala R. Fibrocytes in health and disease. Exp Hematol. 2010;38:548–56.

8. Delprat B, Ruel J, Guitton MJ, Hamard G, Lenior M, Pujol R, Puel JL, Brabet P, Hamel CP. Deafness and cochlear fibrocyte alterations in mice deficient for the inner ear protein otospiralin. Mol Cell Biol. 2005;25:847–53.
9. Hong KM, Belperio JA, Keane MP, Burdick MD, Strieter RM. Differentiation of human circulating fibrocytes as mediated by transforming growth factor-beta and peroxisome proliferators-activated receptor gamma. J Biol Chem. 2007;282:22910–20.
10. Pilling D, Fan T, Huang D, Kaul B, Gomer RH. Identification of markers that distinguish monocyte-derived fibrocytes from monocytes, macrophages, and fibroblasts. PLoS One. 2009; 4:e7475.
11. Sakai N, Wada T, Yokoyama H, Lipps M, Ueha S, Matsushima K, Kaneko S. Secondary lymphoid tissue chemokine (SLC/CCL21)/CCR7 signaling regulates fibrocytes in renal fibrosis. Proc Natl Acad Sci USA. 2006;103:14098–103.
12. Sakai N, Furuichi K, Shinozaki Y, Yamauchi H, Toyama T, Kitajima S, Okumura T, Kokubo S, Kobayashi M, Takasawa K, Takeda S, Yoshimura M, Kaneko S, Wada T. Fibrocytes are involved in the pathogenesis of human chronic kidney disease. Hum Pathol. 2010;41:672–8.
13. Moore BB, Kolodsick JE, Thannickal VJ, Cooke K, Moore TA, Hogaboam C, Wilke CA, Toews GB. CCR2-mediated recruitment of fibrocytes to the alveolar space after fibrotic injury. Am J Pathol. 2005;166:675–84.
14. Phillips RJ, Burdick MD, Hong K, Lutz MA, Murray LA, Xue YY, Belperio JA, Keane MP, Strieter RM. Circulating fibrocytes traffic to the lungs in response to CXCL12 and mediate fibrosis. J Clin Invest. 2004;114:438–46.
15. Ishida Y, Kimura A, Kondo T, Hayashi T, Ueno M, Takakura N, Matsushima K, Mukaida N. Essential roles of the CC chemokine ligand 3-CC chemokine receptor 5 axis in bleomycin-induced pulmonary fibrosis through regulation of macrophage and fibrocyte infiltration. Am J Pathol. 2007;170:843–54.
16. Abe R, Donnelly SC, Peng T, Bulaca R, Metz CN. Peripheral blood fibrocytes: differentiation pathway and migration to wound sites. J Immunol. 2001;166:7556–62.
17. Sakai N, Wada T, Iwai M, Horiuchi M, Matsushima K, Kaneko S. The renin–angiotensin system contributes to renal fibrosis through regulation of fibrocytes. J Hypertens. 2008;26:780–90.
18. Moeller A, Gilpin SE, Ask K, Cox G, Cook D, Gauldie J, Margetts PJ, Farkas L, Dobranowski J, Boylan C, O'Byrne PM, Strieter RM, Kolb M. Circulating fibrocytes are an indicator of poor prognosis in idiopathic pulmonary fibrosis. Am J Respir Crit Care Med. 2009;79:588–94.
19. Ricardo SD, van Goor H, Eddy AA. Macrophage diversity in renal injury and repair. J Clin Invest. 2008;118:3522–30.
20. Ninichunk V, Anders HJ. Bone marrow-derived progenitor cells and renal fibrosis. Front Biosci. 2008;13:5163–7.
21. Sakai N, Wada T, Furuichi K, Shimizu K, Kokubo S, Hara A, Yamahana J, Okumura T, Matsushima K, Yokoyama H, Kaneko S. MCP-1/CCR2-dependent loop for fibrogenesis in human peripheral CD14-positive monocytes. J Leukoc Biol. 2006;79: 555–63.
22. Wada T, Yokoyama H, Su SB, Mukaida N, Iwano M, Dohi K, Takahashi Y, Sasaki T, Furuichi K, Segawa C, Hisada Y, Ohta S, Takasawa K, Kobayashi K, Matsushima K. Monitoring urinary levels of monocyte chemotactic and activating factor reflects disease activity of lupus nephritis. Kidney Int. 1996;49:761–7.
23. Wada T, Yokoyama H, Furuichi K, Kobayashi K, Harada K, Naruto M, Su SB, Akiyama M, Mukaida N, Matsushima K. Intervention of crescentic glomerulonephritis by antibodies to monocyte chemotactic and activating factor (MCAF/MCP-1). FASEB J. 1996;10:1418–25.
24. Wada T, Furuichi K, Segawa C, Shimizu M, Sakai N, Takeda S, Takasawa K, Kida H, Kobayashi K, Mukaida N, Ohmoto Y, Matsushima K, Yokoyama H. MIP-1α and MCP-1 contribute crescents and interstitial lesions in human crescentic glomerulonephritis. Kidney Int. 1999;56:995–1003.
25. Wada T, Furuichi K, Sakai N, Iwata Y, Yoshimoto K, Shimizu M, Takeda S, Takasawa K, Yoshimura M, Kida H, Kobayashi KI, Mukaida N, Naito T, Matsushima K, Yokoyama H. Up-regulation of monocyte chemoattractant protein-1 in tubulointerstitial lesions of human diabetic nephropathy. Kidney Int. 2000;58: 1492–8.
26. Wu X, Dolecki GJ, Sherry B, Zagorski J, Lefkowith JB. Chemokines are expressed in a myeloid cell-dependent fashion and mediate distinct functions in immune complex glomerulonephritis in rat. J Immunol. 1997;158:3917–24.
27. Wada T, Furuichi K, Sakai N, Iwata Y, Kitagawa K, Ishida Y, Kondo T, Hashimoto H, Ishiwata Y, Mukaida N, Tomosugi N, Matsushima K, Egashira K, Yokoyama H. Gene therapy via blockade of monocyte chemoattractant protein-1 for renal fibrosis. J Am Soc Nephrol. 2004;15:940–8.
28. Kitagawa K, Wada T, Furuichi K, Hashimoto H, Ishiwata Y, Asano M, Takeya M, Kuziel WA, Matsushima K, Mukaida N, Yokoyama H. Blockade of CCR2 ameliorates progressive fibrosis in kidney. Am J Pathol. 2004;165:237–46.
29. Furuichi K, Gao JL, Murphy PM. Chemokine receptor CX3CR1 regulates renal interstitial fibrosis after ischemia-reperfusion injury. Am J Pathol. 2006;169:372–87.
30. Rao VH, Meehan DT, Delimont D, Nakajima M, Wada T, Gratton MA, Cosgrove D. Role for macrophage metalloelastase in glomerular basement membrane damage associated with alport syndrome. Am J Pathol. 2006;169:32–46.
31. Tapmeier TT, Fearn A, Brown K, Chowdhury P, Sacks SH, Sheerin NS, Wong W. Pivotal role of CD4+ T cells in renal fibrosis following ureteric obstruction. Kidney Int. 2010;78: 351–62.
32. Nikolic-Paterson DJ. CD4+ T cells: a potential player in renal fibrosis. Kidney Int. 2010;78:333–5.
33. Grande MT, López-Novoa JM. Fibroblast activation and myofibroblast generation in obstructive nephropathy. Nat Rev Nephrol. 2009;5:319–28.
34. Zeisberg M, Duffield JS. Resolved: EMT produces fibroblasts in the kidney. J Am Soc Nephrol. 2010;21:1247–53.
35. Liu Y. New insights into epithelial–mesenchymal transition in kidney fibrosis. J Am Soc Nephrol. 2010;21:212–22.
36. Li J, Qu X, Bertram JF. Endothelial–myofibroblast transition contributes to the early development of diabetic renal interstitial fibrosis in streptozotocin-induced diabetic mice. Am J Pathol. 2009;175:1380–8.
37. Kizu A, Medici D, Kalluri R. Endothelial–mesenchymal transition as a novel mechanism for generating myofibroblasts during diabetic nephropathy. Am J Pathol. 2009;175:371–3.
38. Bechtel W, McGoohan S, Zeisberg EM, Müller GA, Kalbacher H, Salant DJ, Müller CA, Kalluri R, Zeisberg M. Methylation determines fibroblast activation and fibrogenesis in the kidney. Nat Med. 2010;16:544–50.
39. Humphreys BD, Lin SL, Kobayashi A, Hudson TE, Nowlin BT, Bonventre JV, Valerius MT, McMahon AP, Duffield JS. Fate tracing reveals the pericyte and not epithelial origin of myofibroblasts in kidney fibrosis. Am J Pathol. 2010;176:85–97.
40. Lin SL, Kisseleva T, Brenner DA, Duffield JS. Pericytes and perivascular fibroblasts are the primary source of collagen-producing cells in obstructive fibrosis of the kidney. Am J Pathol. 2008;173:1617–27.

Diabetologia
DOI 10.1007/s00125-010-2028-x

ARTICLE

Glucagon-like peptide-1 receptor agonist ameliorates renal injury through its anti-inflammatory action without lowering blood glucose level in a rat model of type 1 diabetes

R. Kodera · K. Shikata · H. U. Kataoka · T. Takatsuka · S. Miyamoto · M. Sasaki · N. Kajitani · S. Nishishita · K. Sarai · D. Hirota · C. Sato · D. Ogawa · H. Makino

Received: 4 June 2010 / Accepted: 30 November 2010

Abstract
Aims/hypothesis Glucagon-like peptide-1 (GLP-1) has various extra-pancreatic actions, in addition to its enhancement of insulin secretion from pancreatic beta cells. The GLP-1 receptor is produced in kidney tissue. However, the direct effect of GLP-1 on diabetic nephropathy remains unclear. Here we demonstrate that a GLP-1 receptor agonist, exendin-4, exerts renoprotective effects through its anti-inflammatory action via the GLP-1 receptor without lowering blood glucose.
Methods We administered exendin-4 at 10 μg/kg body weight daily for 8 weeks to a streptozotocin-induced rat model of type 1 diabetes and evaluated their urinary albumin excretion, metabolic data, histology and morphometry. We also examined the direct effects of exendin-4 on glomerular endothelial cells and macrophages in vitro.
Results Exendin-4 ameliorated albuminuria, glomerular hyperfiltration, glomerular hypertrophy and mesangial matrix expansion in the diabetic rats without changing blood pressure or body weight. Exendin-4 also prevented macrophage infiltration, and decreased protein levels of intercellular adhesion molecule-1 (ICAM-1) and type IV collagen, as well as decreasing oxidative stress and nuclear factor-κB activation in kidney tissue. In addition, we found that the GLP-1 receptor was produced on monocytes/macrophages and glomerular endothelial cells. We demonstrated that in vitro exendin-4 acted directly on the GLP-1 receptor, and attenuated release of pro-inflammatory cytokines from macrophages and ICAM-1 production on glomerular endothelial cells.
Conclusions/interpretation These results indicate that GLP-1 receptor agonists may prevent disease progression in the early stage of diabetic nephropathy through direct effects on the GLP-1 receptor in kidney tissue.

Keywords Anti-inflammatory effect · Diabetic nephropathy · Exendin-4 · Glomerular endothelial cells · GLP-1 receptor agonist · Intercellular adhesion molecule-1 · Macrophage · Nuclear factor-κB · Type 1 diabetic rats

Abbreviations

GLP-1	Glucagon-like peptide-1
GLP-1R	Glucagon-like peptide-1 receptor
hGECs	Human glomerular microvascular endothelial cells
ICAM-1	Intercellular adhesion molecule-1
NOX4	NADPH oxidase 4
NF-κB	Nuclear factor-κB
8-OHdG	8-Hydroxydeoxyguanosine

Electronic supplementary material The online version of this article (doi:10.1007/s00125-010-2028-x) contains supplementary material, which is available to authorised users.

R. Kodera · K. Shikata (✉) · H. U. Kataoka · T. Takatsuka · S. Miyamoto · M. Sasaki · N. Kajitani · S. Nishishita · K. Sarai · D. Hirota · C. Sato · H. Makino
Department of Medicine and Clinical Science,
Okayama University Graduate School of Medicine, Dentistry, and Pharmaceutical Sciences,
2-5-1 Shikata-cho,
Okayama 700-8558, Japan
e-mail: shikata@md.okayama-u.ac.jp

C. Sato · D. Ogawa
Department of Diabetic Nephropathy, Okayama University Graduate School of Medicine, Dentistry, and Pharmaceutical Sciences,
Okayama, Japan

Published online: 21 January 2011

Introduction

The number of patients with diabetes is increasing dramatically throughout the world, while diabetic nephropathy is the leading cause of end-stage renal disease in developed countries. In addition, chronic kidney disease contributes to development of cardiovascular disease and leads to an increase in all-cause mortality rates [1, 2]. Therefore, prevention of renal insufficiency improves the prognosis of diabetic patients.

Numerous factors contribute to the development of diabetic nephropathy, such as glomerular hyperfiltration [3], which is mainly observed in early-stage nephropathy, oxidative stress [4], accumulation of AGEs [5], activation of protein kinase C [6], acceleration of the polyol pathway and overexpression of TGF-β [7]. Accumulating evidence also points to the critical role of the inflammatory process in the development of diabetic vascular complications, suggesting that microinflammation is a common mechanism in pathogenesis of diabetic nephropathy [8, 9]. Furuta et al. [10] reported that infiltration of mononuclear cells was prominent in the glomeruli of patients with diabetic nephropathy. Our group has also reported similar results, as well as observing an increase in the production of cell adhesion molecules in the kidney of diabetic patients [11]. We found that intercellular adhesion molecule-1 (ICAM-1) played a key role in promoting macrophage infiltration in glomeruli from a rat model of diabetes [12], and using mice deficient in ICAM-1, we also showed that blockade of ICAM-1 activation ameliorated diabetic nephropathy [13]. Additionally, we showed that methotrexate, an immunosuppressant, ameliorated diabetic nephropathy and that anti-inflammatory agents also had a beneficial effect on diabetic nephropathy [14]. Modulation of the inflammatory process prevents renal injury in animal models of diabetes, suggesting that microinflammation is a potential therapeutic target in diabetic nephropathy [14–17].

Glucagon-like peptide-1 (GLP-1) is a gut incretin hormone and currently considered an attractive agent for treatment of type 2 diabetes. It has various beneficial effects on pancreatic beta cells, such as enhancement of glucose-dependent insulin secretion [18], acceleration of beta cell proliferation and inhibition of beta cell apoptosis [19]. In the gut and hypothalamus, GLP-1 inhibits motility, gastric emptying [20] and central regulation of feeding [21], resulting in body weight loss [18]. However, native GLP-1 is rapidly degraded in the circulation by dipeptidylpeptidase-IV [22]. Today, dipeptidylpeptidase-IV-resistant, long-acting GLP-1 receptor (GLP-1R) agonists such as exendin-4 and liraglutide are available for type 2 diabetic patients. Previous reports have shown that GLP-1R is produced not only in the pancreas, gut and hypothalamus, but also in the kidney [23–25]. With respect to the effects of GLP-1 on the kidney, it has been reported that exendin-4 ameliorated hypertension by regulating sodium excretion in tubular cells [26] and attenuated renal injury by improving metabolic anomalies in a mouse model of type 2 diabetes [25]. From these results, the amelioration of hypertension and metabolic anomalies by GLP-1 would seem to have a beneficial effect on diabetic nephropathy. In the present study, we focused on the direct effect of GLP-1 through GLP-1R in the kidney, independently of the numerous other effects of GLP-1, including its glucose-lowering action.

Methods

Animals

Male Sprague–Dawley rats (5 weeks old; Charles River, Yokohama, Japan) were divided into the following groups: (1) non-diabetes (n=5); (2) non-diabetes treated with exendin-4 (n=6); (3) diabetes (n=6); and (4) diabetes treated with exendin-4 (n=6). At the age of 5 weeks, the groups allocated to be made diabetic received intravenous injections of streptozotocin (Sigma-Aldrich, St Louis, MO, USA) at 65 mg/kg body weight in citrate buffer (pH 4.5). We included only rats with blood glucose concentrations >16 mmol/l at 3 and 7 days after streptozotocin injection in the diabetes groups. The non-diabetic groups received injections of citrate buffer alone. The two groups treated with exendin-4 were given exendin-4 (Bachem, Bubendorf, Switzerland) intraperitoneally at 10 μg/kg body weight daily for 8 weeks, starting at 1 week after the streptozotocin or citrate buffer injections. The placebo groups were given water alone using the same schedule as in the exendin-4 treatment groups. All rats had free access to standard chow and tap water. All procedures were performed according to the Guidelines for Animal Experiments at Okayama University Medical School, the Japanese Government Animal Protection and Management Law and the Japanese Government Notification on Feeding and Safekeeping of Animals. All rats were killed at 9 weeks after induction of diabetes in the diabetes groups, and the kidneys were weighed and fixed in 10% (vol./vol.) formalin, or frozen in acetone cooled on dry ice.

Metabolic variables

Systolic BP was measured by tail-cuff plethysmography (Softron, Tokyo, Japan). HbA_{1c} was measured by the HPLC method. Serum creatinine was measured by the 3-hydroxy-2,4,6-triiodobenzoic acid method. Food intake was calculat-

ed as the average over 3 days. Insulin concentration was measured by a rat insulin RIA kit (LincoResearch, St Charles, MO, USA). Urine samples were collected over a 24 h period in individual metabolism cages. Urinary albumin excretion was measured by nephelometry using anti-rat albumin antibody (ICN Pharmaceuticals, Aurora, OH, USA). Creatinine clearance (ml min^{-1} kg^{-1}) was calculated as described previously [15].

Light microscopy

The glomerular tuft area and mesangial matrix index (ratio of the mesangial matrix area/glomerular tuft area) were measured using a software package (Lumina Vision; Mitani, Fukui, Japan) as described previously [13]. Periodic acid–Schiff's reagent staining was used to observe the interstitium of the kidney. Quantitative analysis for all staining was performed in a blinded manner.

Immunoperoxidase staining

Immunoperoxidase staining was performed as described [12, 27]. Primary antibodies were macrophages mouse antibody (ED1, 1:50; Serotec, Oxford, UK), 8-hydroxydeoxyguanosin (8-OHdG) mouse antibody (1:10; JalCA, Shizuoka, Japan), NADPH oxidase 4 (NOX4) rabbit antibody (1:300; Novus Biologicals, Littleton, CO, USA) or GLP-1R rabbit antibody (ab39072, 1:200; Abcam, Tokyo, Japan), all of which were applied for 12 h at 4°C. Secondary antibodies were biotin-labelled anti-mouse or anti-rabbit IgG (Jackson ImmunoResearch, West Grove, PA, USA), which were applied for 60 min at room temperature. The average number of ED1-positive cells per glomerulus was used for the estimation. The ratio of the area stained positive with each of the above antibodies to the glomerular tuft area was calculated with a software package (Lumina Vision).

Immunofluorescence staining

Immunofluorescence staining was performed as described [12]. The primary antibodies were ICAM-1 mouse antibody (1:25; Abcam) or type IV collagen rabbit antibody (1:200; LSL, Tokyo, Japan), which were applied for 60 min at room temperature. Secondary antibodies were FITC-conjugated anti-mouse or anti-rabbit IgG (1:150; Zymed Laboratories, San Francisco, CA, USA), which were applied for 30 min at room temperature. Micrographic fluorescence photos were obtained with a laser-scanning confocal microscope (LSM-510; Carl Zeiss, Jena, Germany). The ICAM-1 and type IV collagen indexes were calculated as described [15].

Double immunofluorescence staining

The primary antibodies were GLP-1R rabbit antibody (1:200; Abcam) and rat endothelial cell antigen (RECA-1, 1:40; Monosan, Uden, the Netherlands), macrophages (ED1, 1:50) mouse antibody, or NOX4 rabbit antibody (1:300), which were applied for 12 h at 4°C. The secondary antibodies were Alexa-Fluor 488-labelled anti-rabbit and 546-labelled anti-mouse IgG (1:400; Invitrogen, Carlsbad, CA, USA), which were applied for 30 min at room temperature. Nuclei were stained with DAPI (Millipore, Tokyo, Japan). The sections were observed under a fluorescence microscope (BZ-800; Keyence, Osaka, Japan).

Quantitative real-time RT-PCR and gene expression

Total RNA was extracted from each sample (the rat renal cortex, glomeruli isolated by a previously reported mechanical sieving technique [28] and cultured cells) using a kit (RNeasy plus Mini; Qiagen, Valencia, CA, USA). Single-strand cDNA was synthesised from the individual samples of total RNA at 1 μg using a kit (GeneAmp RNA PCR-

Table 1 Metabolic variables of four rat groups at 8 weeks

Variable	Non-diabetic		Diabetic	
	Placebo	Exendin-4	Placebo	Exendin-4
Body weight (g)	471±23.5[a]	397±8.3[b]	256±30.5	246±22.9
Food intake (g/day)	27.6±0.9[c,d]	19.3±3.1[a]	44.6±12.5	38.6±0.5
HbA_{1c} (%)	3.7±0.1[a]	3.9±0.1[a]	10.5±0.5	10.0±0.8
Fasting blood glucose (mmol/l)	4.0±0.2[a]	4.9±0.3[a]	26.6±0.9	26.6±2.4
Systolic BP (mmHg)	115±2.6	114±1.5	120±1.3	123±2.6
Relative kidney weight (g/kg)	5.9±0.2[a]	6.1±0.1[a]	11.6±0.7	12.0±0.7

Values are the means ± SEM; $n=5$ animals in the non-diabetic placebo group; $n=6$ animals per group in the three other groups

[a] $p<0.001$ vs diabetes and diabetes + exendin-4 groups; [b] $p<0.01$ vs diabetes and diabetes + exendin-4 groups; [c] $p<0.001$ vs diabetes placebo group; [d] $p<0.05$ vs diabetes plus exendin-4 group

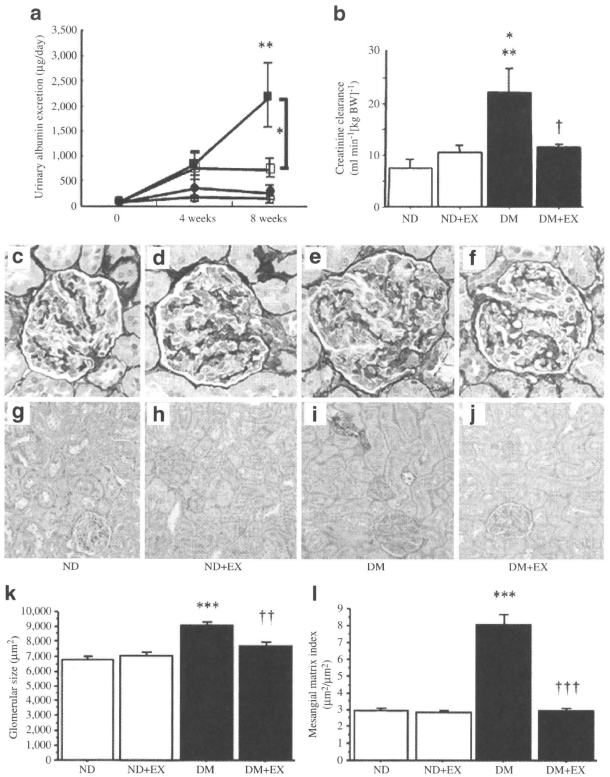

Fig. 1 **a** Time course of 24 h urinary albumin excretion. Urinary albumin excretion increased gradually over 8 weeks in the diabetic group. Exendin-4 resulted in a significantly lower level of urinary albumin excretion at 8 weeks than in the untreated diabetes group. *p <0.05; **p<0.01 vs non-diabetic and non-diabetic + exendin-4 groups. Black circles, non-diabetic group; white circles, non-diabetic + exendin-4; black squares, streptozotocin-induced diabetes group; white squares, diabetes + exendin-4 group. **b** Creatinine clearance. Hyperfiltration in the diabetic (DM) nephropathy group was significantly decreased by exendin-4 treatment (DM+EX) at 8 weeks. *p< 0.05 vs non-diabetic + exendin-4 (ND+EX); **p<0.01 vs ND; †p< 0.05 vs DM. **c–f** Periodic acid–methenamine-silver (PAM) staining in glomeruli (original magnification ×200). **g–j** Periodic acid–Schiff's reagent staining in the kidney (×100). **k** Glomerular size (tuft area). Glomerular hypertrophy was significantly greater in the DM group than in the ND groups. Exendin-4 treatment significantly suppressed glomerular hypertrophy. ***p<0.001 vs ND and ND+EX; ††p<0.01 vs DM. **l** Mesangial matrix index, calculated by the PAM-positive area in the tuft area, was significantly increased in the DM group. Exendin-4 treatment significantly reduced mesangial matrix expansion. ***p< 0.001 vs ND and ND+EX; †††p<0.001 vs DM. n=5 animals in the untreated ND group; n=6 animals per group in the three other groups. **k**, **l** Glomeruli: n=30 from each rat kidney; n=4 per group. Values are the means ± SEM

Core kit; Applied Biosystems, Foster City, CA, USA). After addition of each set of primers (final concentration 0.4 μmol/l) and template DNA to the master mix, quantitative real-time RT-PCR was performed with a LightCycler (Roche Diagnostics, Tokyo, Japan) and SYBR Premix-Ex-Taq (Takara Bio, Shiga, Japan). The PCR protocol was as follows: initial denaturation (95°C for 30 s), followed by 40 cycles of denaturation (95°C for 5 s), and annealing and extension (60°C for 20 s). The specific oligonucleotide primer sequences are shown in

Electronic supplementary material (ESM) Table 1. To visualise gene expression, individual DNA fragments were electrophoresed on a 2% (wt./vol) agarose gel (Sigma-Aldrich) and treated with ethidium bromide. cDNAs of the human pancreas (Takara Bio) and of rat islet-cell tumour cells (RIN-5F; DS Pharma Biomedical, Osaka, Japan) were used as positive controls.

Urinary 8-OHdG excretion

8-OHdG is a marker of oxidative DNA damage [29]. Urinary 8-OHdG concentration in a 24 h urine collection was measured with a kit (8-OHdG ELISA; JalCA) according to the manufacturer's instructions.

Nuclear factor-κB activation

Nuclear proteins of kidney tissues were extracted by a nuclear extract kit and nuclear factor-κB (NF-κB) p65 activity determined by ELISA using reagents (Active-Motif; Carlsbad, CA, USA) according to the manufacturer's instructions. Absorbance was normalised to milligram cell protein.

Western blotting

Cells were lysed with cell lysis buffer containing 10 mmol/l TRIS (pH 7.4), 1% (vol./vol.) Triton X-100, 0.5% (vol./vol.) Nonidet P-40 and phosphatase inhibitor cocktail, 150 mmol/l NaCl, 1 mmol/l EDTA, 0.2 mmol/l EGTA, vanadate and phenylmethanesulfonyl fluoride. The cell lysates were subjected to 7.5% SDS-PAGE (Bio-Rad Japan, Tokyo, Japan). The separated proteins were transferred to polyvinylidene fluoride membranes (Bio-Rad) by electrotransfer. The blots were subsequently blocked with 5% (vol./vol.) skimmed milk (Nacalai Tesque, Kyoto, Japan) and then incubated with GLP-1R rabbit antibody (1:500; Abcam) and ICAM-1 mouse antibody (1:100; Abcam) for 12 h at 4°C, or with β-actin rabbit antibody (1:1,000; Sigma-Aldrich) for 1 h at room temperature. The membrane was incubated with horseradish-peroxidase-linked donkey anti-rabbit or anti-mouse IgG (1:5,000; GE Healthcare Japan, Tokyo, Japan) at room temperature for 2 h. The blots were then visualised with a western blotting detection system (ECL plus; GE Healthcare).

Culture

Human glomerular microvascular endothelial cells (hGECs) (ACBRI, Kirkland, WA, USA) were cultured in EGM-MV2 medium (Cambrex, East Rutherford, NJ, USA) supplemented with 19.4 mmol/l D-glucose, 10% (vol./vol.) FCS and growth factor within a gelatin-precoated flask in a 5% CO_2 incubator at 37°C.

THP-1 cells (a human monocytic cell line; JCRB, Tokyo, Japan) were cultured in RPMI 1640 supplemented with 10 mmol/l D-glucose, 10% FCS and growth factor in a 5% CO_2 incubator at 37°C.

Human circulating monocytes

The human circulating monocytes were extracted using lymphocyte separation medium (MP Biomedicals, Tokyo, Japan) according to the manufacturer's instructions. After incubation in RPMI 1640 with 50 ng/ml phorbol myristate acetate (Sigma-Aldrich) for 24 h, total RNA was collected from the attaching cells as described above.

The effects of GLP-1 in THP-1 cells

THP-1 cells (1×10^6 cells/ml) were incubated for 24 h in six-well plates in RPMI 1640 medium supplemented with 1% FCS and 5.5 mmol/l D-glucose. THP-1 cells were exposed to the following conditions: (1) 5.5 mmol/l D-glucose (normal glucose); (2) 5.5 mmol/l D-glucose with 9.5 mmol/l mannitol (osmotic control); (3) 15 mmol/l D-glucose (high glucose); (4) high glucose with 2.5 nmol/l exendin-4; (5) high glucose with 10 nmol/l exendin-4; (6) high glucose with 100 nmol/l exendin-4; and (7) high glucose with 100 nmol/l exendin-4 and 1000 nmol/l GLP-1R antagonist (9-39) (Bachem). After incubation for 72 h, total RNA and supernatant fractions were collected from the cells. The supernatant fractions were measured using a human TNF-α and IL-1β immunoassay (Quantikine; R&D Systems, Minneapolis, MN, USA) according to the manufacturer's instructions.

The effect of GLP-1 in hGECs

After starvation for 12 h, hGECs were exposed to the following conditions: (1) no TNF-α stimulation (control); (2) 100 pg/ml TNF-α alone; (3) TNF-α with 2.5 nmol/l exendin-4; (4) TNF-α with 10 nmol/l exendin-4; (5) TNF-α with 100 nmol/l exendin-4; and (6) TNF-α with 100 nmol/l exendin-4 and 1000 nmol/l GLP-1R antagonist (9-39). After incubation for 6 h, total RNA and protein were collected from cells as described above. Recombinant human TNF-α was purchased from R&D Systems.

Statistical analysis

All values are expressed as the means ± SEM. Differences between groups were examined for statistical significance using the Mann–Whitney test or one-way ANOVA followed by Scheffe's test. Values of $p<0.05$ were considered to indicate statistically significant differences.

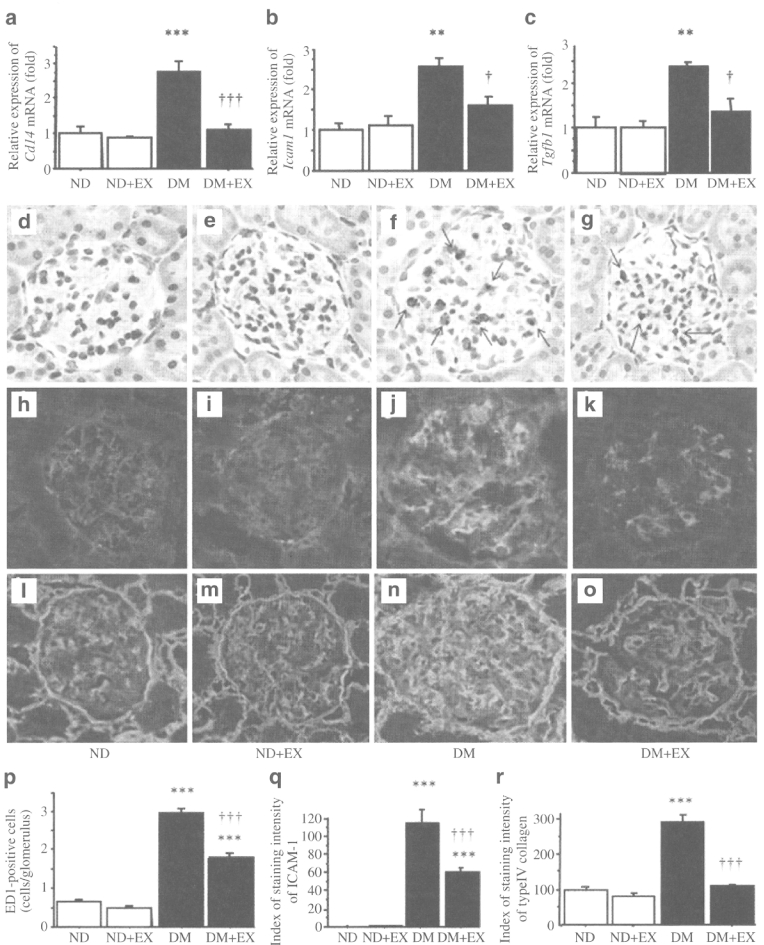

Fig. 2 Exendin-4 treatment suppressed the inflammatory axis in the kidney. **a** Quantification of *Cd14*, (**b**) *Icam1* and (**c**) *Tgfb1* gene expression by real-time RT-PCR in the renal cortex. All three genes were significantly downregulated by exendin-4 treatment. Values (means ± SEM) are presented as fold relative to *Actb* and expressed as 1 in ND; n=4 per group. Each experiment was performed three times. $^{**}p<0.01$ and $^{***}p<0.001$ vs non-diabetic (ND) and ND + exendin-4 (EX); $^{\dagger}p<0.05$ and $^{\dagger\dagger\dagger}p<0.001$ vs diabetes (DM). **d–g** Immunoperoxidase staining for macrophages (ED1-positive cells), indicated by arrows. **h–k** Immunofluorescence staining for ICAM-1 and (**l–o**) for type IV collagen. Magnification, all images ×200. **p** Quantification of the number of macrophages per glomerulus, which was significantly increased in the diabetic groups. Exendin-4 treatment significantly prevented glomerular macrophage infiltration in diabetes. $^{***}p<0.001$ vs ND and ND+EX; $^{\dagger\dagger\dagger}p<0.001$ vs DM. **q** Quantification of glomerular ICAM-1 staining per glomerulus, which was significantly increased in the diabetic groups and significantly reduced vs DM by exendin-4 treatment. $^{***}p<0.001$ vs ND and ND+EX; $^{\dagger\dagger\dagger}p<0.001$ vs DM. **r** Quantification of type IV collagen staining per glomerulus. Type IV collagen was significantly increased in the DM group and significantly reduced by exendin-4 treatment. $^{***}p<0.001$ vs ND and ND+EX; $^{\dagger\dagger\dagger}p<0.001$ vs DM. **p–r** Values are the means ± SEM; n=20 glomeruli from each rat kidney; n=4 per group. Each experiment was repeated three times

Results

Metabolic variables and urinary albumin excretion

Body, organ weights and systolic BP As seen in Table 1, body weights of the diabetic groups at 8 weeks after initiation of exendin-4 treatment were significantly lower than those of the non-diabetic groups. The kidney weights per body weight of the diabetic groups were significantly higher than those of the non-diabetic groups. There were no significant differences among the diabetic groups. Systolic BP was similar in all groups.

Food intake, HbA_{1c} and insulin Food intake and HbA_{1c} were significantly elevated in the diabetic groups. However, there were no significant differences among the diabetic groups. Although GLP-1 has beta cell-protective effects, serum insulin concentration was not detectable in the diabetic groups in spite of the high blood glucose levels (data not shown).

Urinary albumin excretion and creatinine clearance Urinary albumin excretion, which is a characteristic feature of the early stage of diabetic nephropathy, increased progressively in the diabetic groups during the study. Exendin-4 treatment significantly reduced urinary albumin excretion compared with that of the diabetes group at 8 weeks (Fig. 1a). In addition, exendin-4 treatment prevented diabetes-induced hyperfiltration (Fig. 1b).

Kidney morphology

The level of glomerular hypertrophy was significantly higher in the diabetes group than in non-diabetic groups. In contrast, exendin-4 treatment inhibited glomerular hypertrophy (Fig. 1c–f, k) in diabetes. Quantitative analysis showed that mesangial matrix index, which was used as an index of mesangial expansion, was significantly increased in the diabetes group. However, exendin-4 treatment significantly reduced mesangial matrix expansion (Fig. 1l). The renal interstitium showed a significantly higher level of tubular hypertrophy in the diabetic groups than in non-diabetic groups. However, there was no remarkable difference among the diabetic groups. In addition, no histological change of fibrosis in the renal interstitium was seen in any of the groups (Fig. 1g–j).

Microinflammation in the kidney

To evaluate the anti-inflammatory effect of exendin-4 in the kidney, we examined gene expression of *Cd14*, which is regarded as a cell surface marker of macrophages, as well as expression of *Icam1* and *Tgfb1* in the cortex. *Cd14*, *Icam1* and *Tgfb1* were significantly upregulated in the diabetes group and significantly downregulated by exendin-4 treatment (Fig. 2a–c). Regarding the glomeruli, we evaluated macrophage infiltration, and ICAM-1 and type IV collagen levels in glomeruli. The number of macrophages in glomeruli was significantly elevated in the diabetic compared with the non-diabetic groups. In contrast, exendin-4 treatment significantly prevented glomerular macrophage infiltration (Fig. 2d–g, p) in diabetes. The ICAM-1 level was significantly increased in the diabetic groups, but was significantly reduced by exendin-4 treatment (Fig. 2h–k, q). The type IV collagen level, which is an important component in the mesangial matrix, was significantly increased in the diabetes group and significantly reduced by exendin-4 treatment (Fig. 2l–o, r).

Influence of exendin-4 on oxidative stress

To evaluate oxidative stress, we focused on 8-OHdG and NOX4. Urinary excretion of 8-OHdG was significantly increased in the diabetic groups compared with the non-diabetic groups. Exendin-4 treatment significantly decreased urinary excretion of 8-OHdG in diabetes (Fig. 3a). Immunoperoxidase staining for 8-OHdG revealed a significant abundance of 8-OHdG in glomeruli in the diabetic groups, which was significantly reduced by exendin-4 treatment (Fig. 3b–e, j). *Nox4* gene expression in the cortex was significantly upregulated in the diabetes group and significantly downregulated by exendin-4 treatment (Fig. 3k). We demonstrated the presence of NOX4 in glomerular endothelial cells in the rat kidney (ESM Fig. 1h–k). Immunoperoxidase staining for NOX4 revealed a significant abundance of NOX4 in the diabetic kidney. However, exendin-4 treatment significantly reduced the level of NOX4 in diabetes (Fig. 3f–i, l).

NF-κB activation in the kidney

The activation of NF-κB p65 DNA-binding activity was significantly enhanced in the diabetes compared with the non-diabetic groups. Exendin-4 treatment significantly inhibited NF-κB p65 DNA-binding activity in diabetes (Fig. 3m).

GLP-1R in rat glomeruli

We demonstrated the existence of GLP-1R in rat glomeruli (Fig. 4a, d). Double immunofluorescence staining revealed production of GLP-1R on glomerular endothelial cells (Fig. 4e–h). In addition, we ascertained that GLP-1R was produced on macrophages in rat glomeruli (Fig. 4i–l). The GLP-1R levels in glomeruli were not significantly different among the groups (ESM Fig. 1a–g).

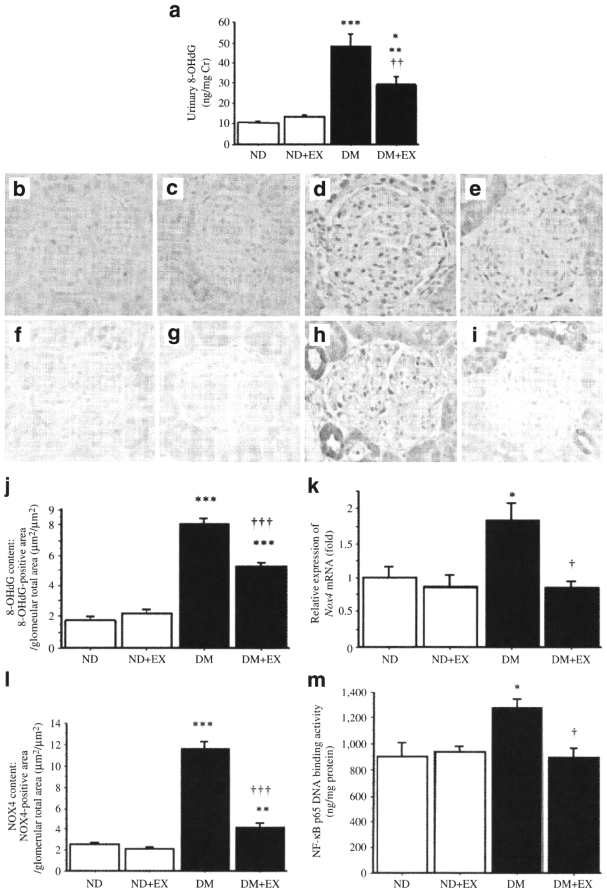

Fig. 3 Exendin-4 treatment suppressed oxidative stress and NF-κB activation. **a** Urinary 8-OHdG concentration in a 24 h urine collection. Urinary 8-OHdG excretion was significantly increased in the diabetic groups (DM). However, exendin-4 treatment (EX) significantly decreased urinary 8-OHdG excretion; $n=5$ per group. The experiment was repeated twice. *$p<0.05$ vs non-diabetic (ND)+EX; **$p<0.01$ vs ND; ***$p<0.001$ vs ND and ND+EX; $^{\dagger\dagger}p<0.01$ vs DM. **b–e** Immunoperoxidase staining for 8-OHdG and (**f–i**) NOX4 in glomeruli. Magnification, all images ×200. **j** Quantification of 8-OHdG content ($\mu m^2/\mu m^2$) as staining per glomerulus. Glomerular 8-OHdG content was significantly increased in the diabetic groups and significantly reduced by exendin-4 treatment. Values are means ± SEM; $n=20$ glomeruli from each rat kidney; $n=4$ per group. ***$p<0.001$ vs ND and ND+EX; $^{\dagger\dagger\dagger}p<0.001$ vs DM. **k** Quantification of *Nox4* by real-time RT-PCR in the renal cortex. *Nox4* expression was significantly downregulated by exendin-4 treatment. Values (means ± SEM) are presented as fold relative to *Actb* and expressed as 1 in ND; $n=4$ per group. Each experiment was repeated three times. *$p<0.05$ vs ND and ND+EX; $^{\dagger}p<0.05$ vs DM. **l** Quantification of NOX4 content ($\mu m^2/\mu m^2$) as staining per glomerulus. NOX4 content was significantly increased in the diabetic groups and significantly suppressed by exendin-4 treatment. Values are means ± SEM; $n=20$ glomeruli from each rat kidney; $n=4$ per group. **$p<0.01$ and ***$p<0.001$ vs ND and ND+EX; $^{\dagger\dagger\dagger}p<0.001$ vs DM. **m** NF-kB p65 DNA-binding activity. NF-κB p65DNA-binding activity was significantly increased in the DM group. Exendin-4 treatment significantly decreased NF-κB p65 DNA-binding activity. Values are the means ± SEM; $n=5$ per group. The experiment was repeated twice. *$p<0.05$ vs ND and ND+EX; $^{\dagger}p<0.05$ vs DM

GLP-1R in human macrophages and hGECs

We identified the existence of GLP-1R in THP-1 cells and hGECs (Figs 5a, b and 6a, b). In addition, we examined *GLP1R* gene expression in human circulating monocytes. We demonstrated that the *GLP-1R* gene was not only expressed in the THP-1 cell line, but also in human circulating monocytes (Fig. 5a).

The effects of GLP-1 through GLP-1R on THP-1 cells and hGECs

THP-1 cells stimulated with a high concentration of glucose for 72 h showed significantly enhanced levels of *TNF* and *IL1B* gene expression. Exendin-4 significantly and dose-dependently attenuated *TNF* and *IL1B* gene expression. Additionally, the effects of exendin-4 were significantly blocked by a GLP-1R antagonist (Fig. 5c, d). Similarly, exendin-4 significantly suppressed TNF-α and IL-1β secretion from THP-1, effects that were also significantly blocked by the GLP-1R antagonist (Fig. 5e, f).

hGECs stimulated with TNF-α for 6 h showed significantly enhanced *ICAM1* gene expression. Exendin-4 significantly and dose-dependently attenuated *ICAM1* gene expression. In addition, the effect of exendin-4 was significantly blocked by the GLP-1R antagonist (Fig. 6c). Likewise, exendin-4 significantly suppressed TNF-α-induced ICAM-1 production on hGECs, an effect that, again, was also significantly blocked by the GLP-1R antagonist (Fig. 6d, e).

Discussion

In the present study, we showed that exendin-4 exerted renoprotective effects through anti-inflammatory actions without lowering the blood glucose level in a streptozotocin-induced rat model of type 1 diabetes. In addition, exendin-4 inhibited NF-κB activity in the kidney, which is known to contribute to cross-talk between inflammation and oxidative stress. We also found that GLP-1R was produced in rat, and in cultured macrophages and glomerular endothelial cells. Exendin-4 acted directly on GLP-1R and attenuated production of pro-inflammatory cytokines and ICAM-1 in vitro. This is the first report of a GLP-1R agonist directly contributing, via its anti-

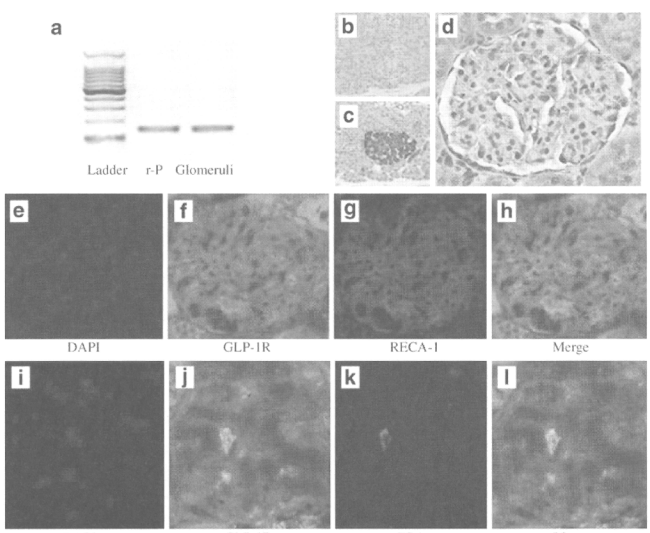

Fig. 4 The production of GLP-1R in rat glomeruli. **a** *Glp1r* gene expression in rat glomeruli. r-P: rat positive control (RIN-5F: rat islet-cell tumour). **b** Immunoperoxidase staining for GLP-1R, with negative control in rat pancreas islet cells, (**c**) positive control in rat pancreas islet cells and (**d**) rat glomeruli. **e–h** Double immunofluorescence staining for GLP-1R and glomerular endothelial cells as labelled. RECA-1, rat endothelial cell antigen. **i–l** Double immunofluorescence staining for GLP-1R and macrophages

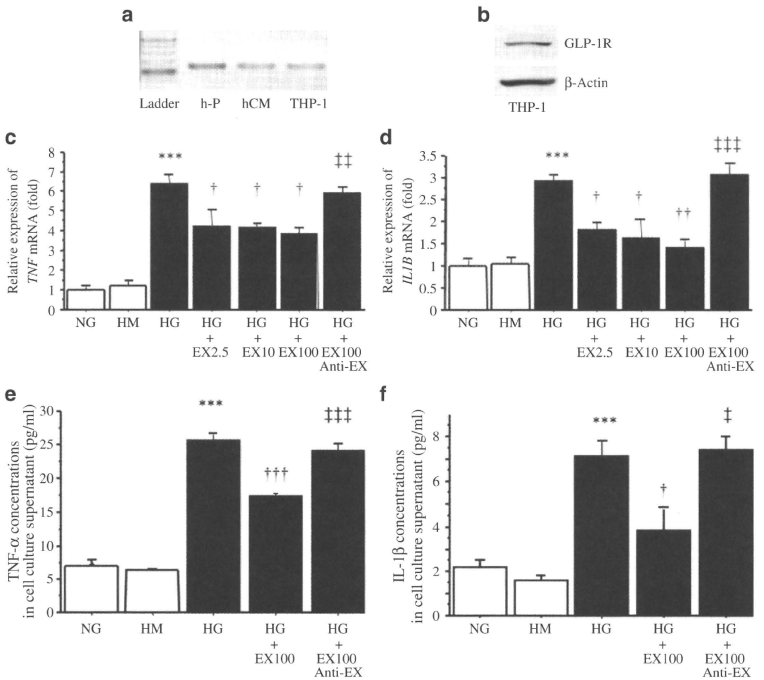

Fig. 5 The direct effects of exendin-4 on THP-1 cells. **a** *GLP1R* gene expression in human circulating monocytes (hCM) and THP-1 cells. h-P, human positive control (human pancreas). **b** GLP-1R protein production in THP-1 cells by western blotting. **c** Quantification of *TNF* and (**d**) *IL1B* mRNA expression in THP-1 by real-time RT-PCR. THP-1 cells stimulated with 15 mmol/l high glucose (HG; 15.0 mmol/l D-glucose) for 72 h showed significantly enhanced *TNF* and *IL1B* expression. Exendin-4 (EX) significantly and dose-dependently suppressed *TNF* and *IL1B* gene expression. GLP-1R antagonist (anti-EX; 1,000 nmol/l) significantly inhibited the suppressive effects of exendin-4 (100 nmol/l) on *TNF* and *IL1B* expression. Values (means ± SEM) are presented as fold relative to *GAPDH* and expressed as 1 in normal glucose (NG; 5.5 mmol/l D-glucose), $n=5$ per group. The experiment was repeated three times. ***$p<0.001$ vs NG and 5.5 mmol/l D-glucose with 9.5 mmol/l mannitol (HM); $^{\dagger}p<0.05$ and $^{\dagger\dagger}p<0.01$ vs HG; $^{\ddagger\ddagger}p<0.01$ and $^{\ddagger\ddagger\ddagger}p<0.001$ vs HG+EX (100 nmol/l; EX100). **e** Quantification of TNF-α and (**f**) IL-1β secretion (pg/ml) from THP-1 by ELISA. Stimulation of THP-1 cells with HG for 72 h significantly promoted TNF-α and IL-1β secretion. Exendin-4 significantly suppressed TNF-α and IL-1β secretion. GLP-1R antagonist (anti-EX; 1,000 nmol/l) significantly inhibited the suppressive effects of exendin-4 (100 nmol/l) on TNF-α and IL-1β secretion. Values are the means ± SEM; $n=5$ per group. The experiment was repeated twice. ***$p<0.001$ vs NG and HM; $^{\dagger}p<0.05$ and $^{\dagger\dagger\dagger}p<0.001$ vs HG; $^{\ddagger}p<0.05$ and $^{\ddagger\ddagger\ddagger}p<0.001$ vs HG+EX100. EX2.5, 2.5 nmol/l exendin-4; EX10, 10 nmol/l exendin-4

inflammatory effects, to amelioration of characteristic features of diabetic nephropathy, such as increased urinary albumin excretion, glomerular hypertrophy and mesangial matrix expansion.

The current results suggest that exendin-4 alleviated the above-mentioned features by suppressing: (1) ICAM-1 production; (2) macrophage infiltration; (3) NF-κB activation; (4) oxidative stress; and (5) *Tgfb1* mRNA expression and type IV collagen accumulation in the kidney.

An increase in the level of ICAM-1 on glomerular endothelial cells promotes macrophage infiltration into glomeruli [12, 14]. In our study, exendin-4 prevented macrophage infiltration into glomeruli. The mechanism underlying this effect was thought to be the suppression of ICAM-1 production on glomerular endothelial cells and direct inhibition of cytokine release from macrophages, which breaks the vicious cycle between macrophages and glomerular endothelial cells that gives rise to microinflam-